

# The Effect of Physical Changes in a Furnished Indoor Environment on Wireless Local Area Network (wlan) Signals

E. M. Cheng

*School of Mechatronic Engineering, Universiti Malaysia Perlis, 02600, UniMAP Perlis, Malaysia.*  
emcheng@unimap.edu.my

Zulkifly Abbas

*Department of Physics, Faculty of Science, Universiti Putra Malaysia, 43400 UPM Serdang, Malaysia,*  
za@science.upm.edu.my

M. Fareq S. F. Khor

*School of Electrical Systems Engineering, Universiti Malaysia Perlis, 02000, UniMAP, Perlis. Malaysia,*  
mfareq@unimap.edu.my; sfkhor@unimap.edu.my;

K. Y. You

*Department of Radio Communication Engineering, Faculty of Electrical Engineering, Universiti Teknologi Malaysia, 81310 UTM Skudai, Malaysia,*  
kyyou@fke.utm.my

K. Y. Lee,

*Department of Electrical and Electronic Engineering, Faculty of Engineering and Science, Universiti Tunku Abdul Rahman, 46200, UTAR Selangor, Malaysia,*  
kylee@utar.edu.my

Abdul Majid, M. S., Rojan M. A.

*School of Mechatronic Engineering, Universiti Malaysia Perlis, 02600, UniMAP Perlis. Malaysia,*  
shukry@unimap.edu.my, afendirojan@unimap.edu.my

\* Corresponding author: Ee Meng Cheng (emcheng@unimap.edu.my).

**Abstract-- This paper describes the investigation of the effect on the Wireless Local Area Network (WLAN) signals due to fixed and non-fixed variables in indoor environment. The measurement system consisted of a spectrum analyzer and a log-periodic antenna. Line-of-sight (LOS) and non-line-of-sight (NLOS) propagation (in furnished rooms) were discussed. All the measurement sites mentioned in this paper are located in the Division of Information Technology at Universiti Putra Malaysia. The furnished rooms included a teaching laboratory, a computer laboratory, and an operating office plus a server room. The effects of the various types of materials at the measurement sites also are described here.**

## 1. INTRODUCTION

Access to information has become a necessity. The information available on the Internet and the easy access to this information allow professionals to utilize tools that would not have been available without this communication facility. As a result, the Internet has become an indispensable tool as well as an open window for people to display their information to the world.

For the sake of quality wireless access to the Internet, service providers must install WLAN systems that can perform optimally. Therefore, it is necessary to develop a proper measurement system to analyze the propagation characteristics of the indoor environment. The installation of a WLAN system should be conducted after the analysis of the

indoor environment's propagation characteristics. Such an analysis will help to ensure that WLAN signal provides optimum coverage throughout the building [1].

Actually, the indoor propagation of radio signals is weather independent, which is unlike outdoor propagation. However, the layout of a building and especially the construction materials used can have significant effects on the propagation of signals [2]. In addition, multipath fading due to obstacles in the building also must be taken into account [3]. The characteristics of the propagation path for indoor communication systems are very unique compared to outdoor systems because various obstacles, e.g. wall, ceiling, floor, and furniture, can reflect, diffract, or shadow the radio waves. Reflections from obstacles and their path differences are unpredictable since people are frequently moving around in the office space.

Measuring indoor signals differs from measuring outdoor signals in that, indoors, the distances are much shorter, and the uncertainty of the environment is much greater for the shorter distances between the transmitter and the receiver. Many research reported that propagation within buildings is influenced significantly by several factors, including the layout of the building, the construction materials, the arrangement of obstacles, and the type of building. In addition, signal levels are affected significantly by the movement of

people, where the antenna is mounted, and the opening and closing of doors. These features inside the office are categorized as fixed and non-fixed variables. and they are discussed in more detail in Section 3.

## 2. METHODOLOGY

### 2.1 Experimental Setup

The measurement of field strength is conducted by using the appropriate apparatus, i.e. an ADVANTEST U3641 spectrum analyzer, in conjunction with an AHS/SAS-519-4 log periodic antenna.

### 2.2 Measurement sites (Division of Information Technology)

The Division of Information Technology is the operating center that manages the entire Internet network at Universiti Putra Malaysia (UPM). The Division of Information Technology was chosen as the site for measurements in this project because WLAN service is provided inside the building that houses the Division. The location of the antenna and measurement Site A, B, C, D and E are shown in Figure 1. As shown in Figure 2 and 3, the antenna was mounted on the ceiling, which is 2.58 m from the floor.

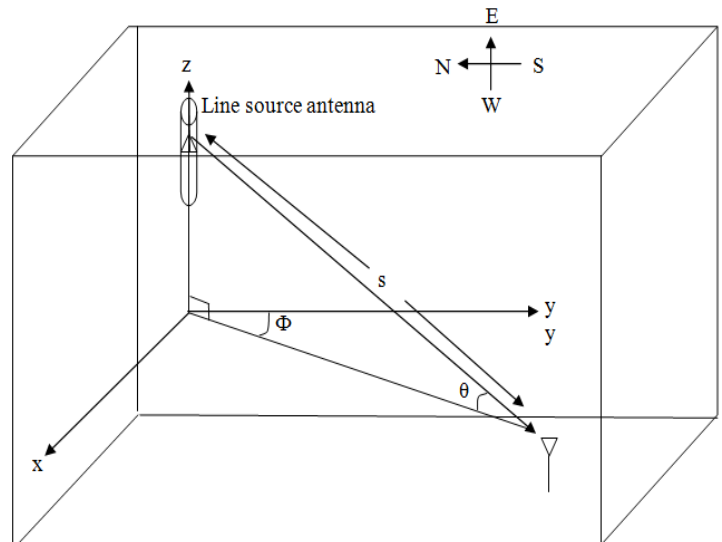


Fig. 2. Coordinates of the propagation system in the indoor environment



Fig. 3. Magnetically-Mounted Omni Antenna (2.4 GHz, 5 dBi)

(a) Site A, B and E

Sites A, B and E are teaching laboratories that are furnished; 20 computers were provided for these measuring sites. Two concrete pillars are located at the center of each of the laboratories, and they were the main causes for losses in the signal strength of the signals. Glass walls divided Site A, B and E from Site C (the location of the transmitter/antenna). Five positions were selected for taking measurements in Site A, B and E. (Figure 4).

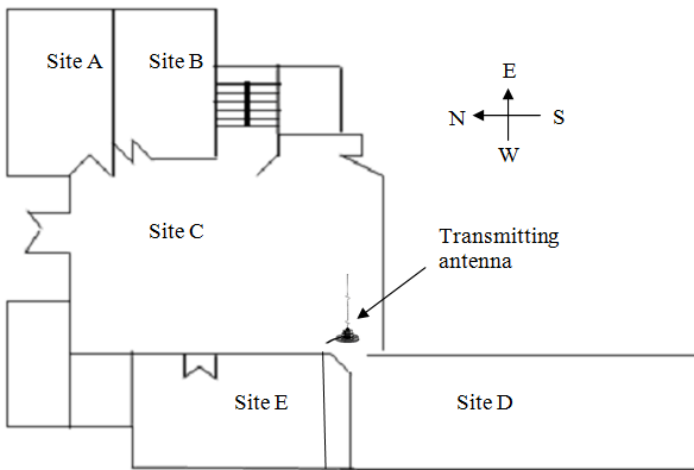


Fig. 1. Antenna and measurement sites

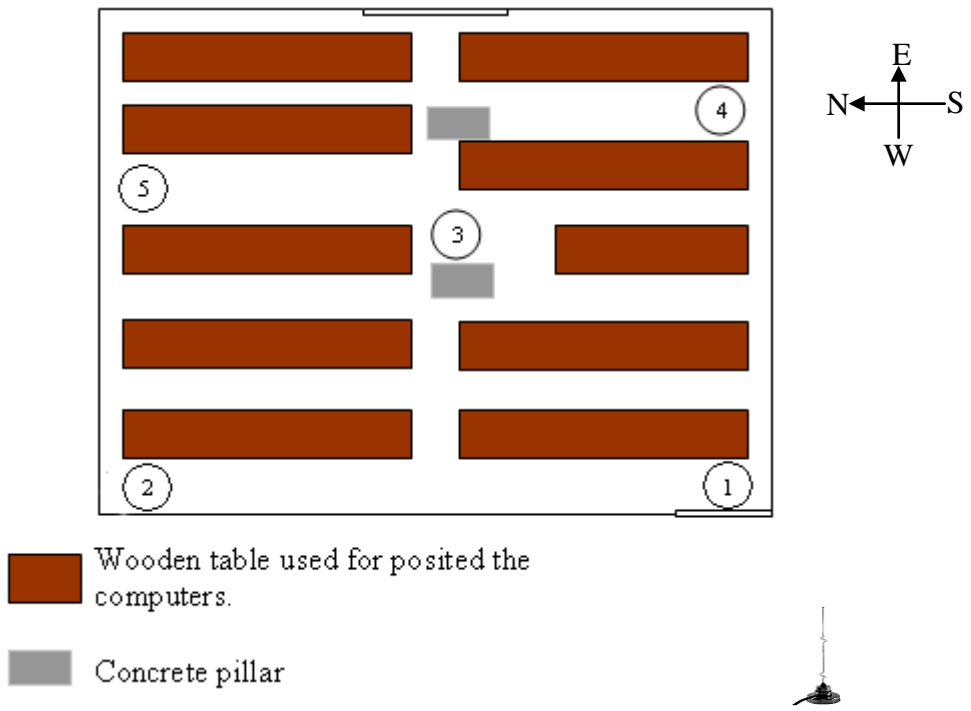


Fig. 4. Plan of Site A

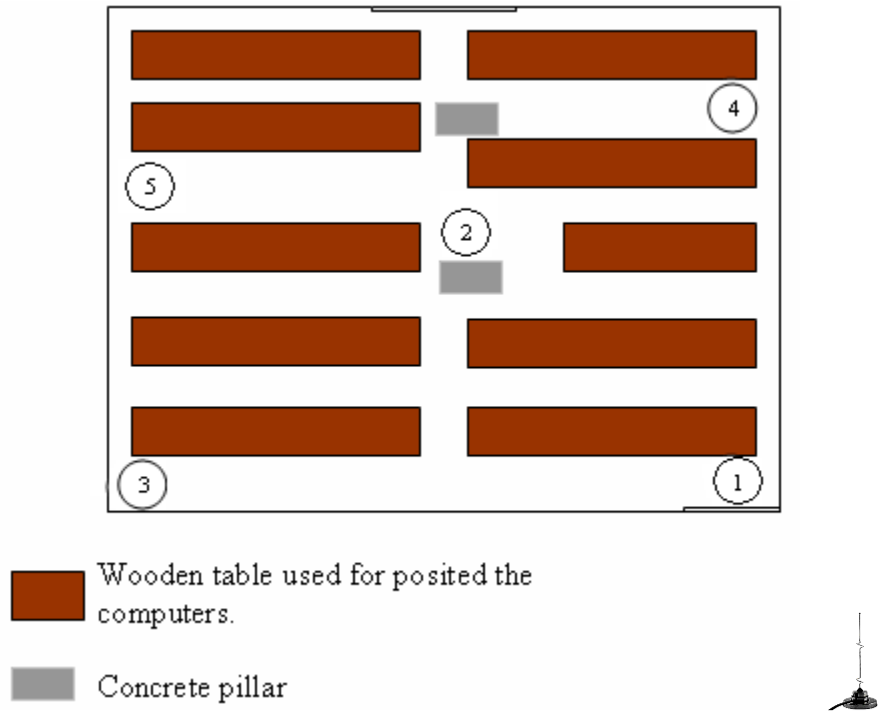


Fig. 5. Plan of Site B

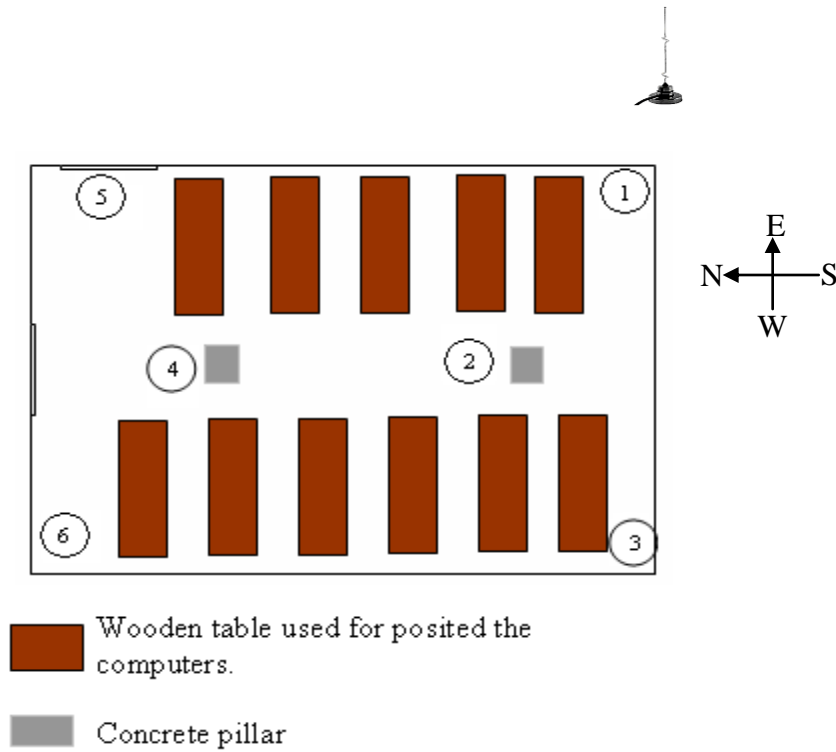


Fig. 6. Plan of Site E

(b) Site C

The foyer of this building was selected as Site C (Figure 7). An antenna was mounted on the ceiling at this site, as shown in Figure 3. The antenna is in the line-of-sight at all of the measuring positions at Site C, and its propagation pattern is as shown in Figure 2. However, in addition to the walls and the ceiling, there were two other obstacles that causes multipath signal, i.e., the round wooden table with a wooden pillar and the wooden shelf. The area of Site C is the largest among all of the sites, so 11 positions were chosen for measurements, as shown in Figure 7.

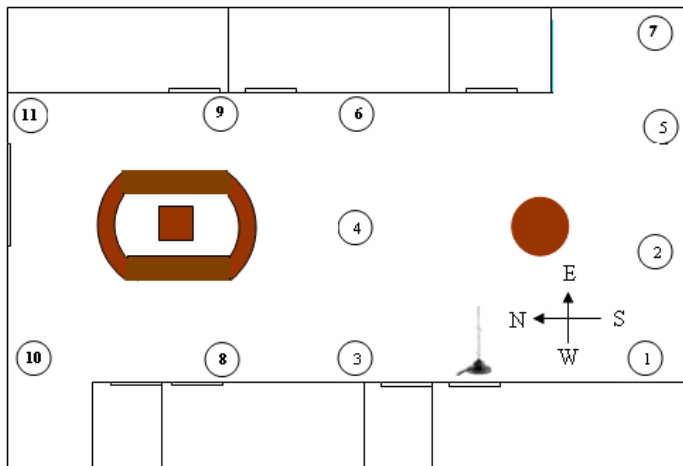


Fig. 7. Plan of Site C

(c) Site D

Site D is the Network Operating Room where five measuring positions were chosen (Figure 8). There are two concrete pillars in the center of the room similar to Site A, B and E. Computers, computer desks, and chairs are located there. There is hard partition in Site D that was not present in Site A, B, C and E.

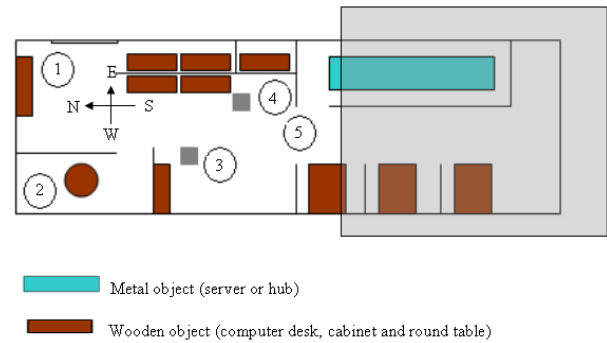


Fig. 8. Plan of Site D

Five positions were chosen as measuring sites in site D. It was found that the signal could not be detected by the spectrum analyzer in the server-room region of Site D (Figure 9), which is represented by the gray area in Figure 8. The gray area is farther from the transmitter than any other part of the Network Operating Room. The corridor after position 5 is like a tunnel (Figure 10). It was assumed that there was no direct signal in the gray shadow region and that the signal was weak (i.e.

negligible) due to multiple reflections that scattered the signals in this region [4].



Fig. 9. Location of the hub or server



Fig. 10. Tunnel-like corridor

### 3. RESULTS AND DISCUSSION

#### 3.1 Performance of the propagation channel regarding the fixed and non-fixed variable

In making the measurement, we had to be sure to take into account both the fixed variable and non-fixed variables.

##### (a) Fixed variables

The fixed variables were the distance, size and orientation of the pillars, walls, floor, ceiling, and tables (unmovable furniture or objects). These fixed variables contributed to significant losses in the WLAN transmission.

##### (b) Non-fixed variables

Four types of non-fixed variables were investigated, i.e., the size of an object, the number of objects, the orientation of objects, and the density of objects. The influence of the non-fixed variables on the strength of the WLAN signal is shown as:

##### (i) Size of object

Table I

The effect of altering the size of an object on the strength of the signal

Object	size / volume of object (m <sup>3</sup> )	signal strength (dB $\mu$ V/m)
Long desk	1.21	14.91
Medium-sized table	0.60	15.09
Small-sized table	0.29	13.88
Chair	0.13	13.60

Table I show that the size of the objects has an insignificant effect on the strength of the signal, as evidenced by the mean and standard error of signal strength, i.e., 14.37 dB  $\mu$ V/m and 0.37 dB  $\mu$ V/m, respectively. The size changes only caused the signal strength to vary by about 2.57 %. Thus, we concluded that changes in the width or length of an object have an insignificant effect on the strength of the signal. However, if the height of an object exceeds a certain limit, the object may block the transmitted signal from reaching the receiving antenna, thereby causing a high attenuation of the signal.

##### (ii) Number of objects

Table II

The effect of changing the number of object on the strength of the signal

Number of objects	Signal strength (dB $\mu$ V/m)
1	14.39
2	14.91
3	16.43
4	16.78
5	16.12
6	16.04
7	14.28
8	13.21
9	14.58

The results were similar in this case to those observed for the sizes of objects. As shown in Table 2, changing the number of objects had little noticeable effect on the strength of the signal at a particular distance. The mean and standard error of the strength of the signal were 15 dB  $\mu$ V/m and 0.40 dB  $\mu$ V/m, respectively. This information indicates that the variability in percentage is only about 2.6 %. This figure is similar to case (i), and it was concluded that the strength of the signal was independent of the sizes of objects (area of the bases of the objects) and the number of objects. However, an exception to this conclusion must be made if objects are placed close to transmitting antenna, where they could cause significant scattering of the signal.

(iii) Orientation of objects

Table III

Effect of different orientations of objects on the strength of the signal

Angle of rotation (anti-clockwise), degrees	Signal strength (dB $\mu\text{V}/\text{m}$ )
0	11.32
15	10.59
30	12.44
45	11.59
60	7.26
75	7.61
90	5.22
105	4.70
120	6.00
135	6.10
150	8.62
165	9.59
180	11.69

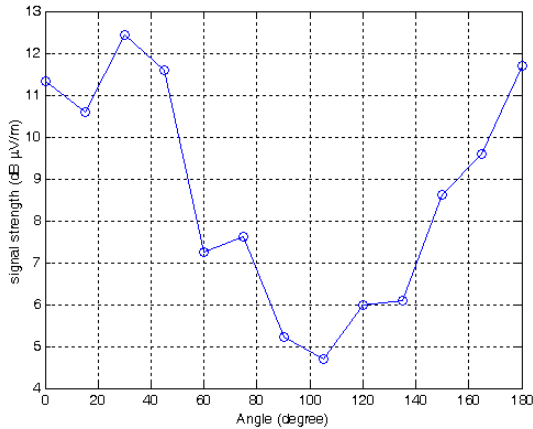


Fig. 11. Change in the strength of the signal with the angle of rotation

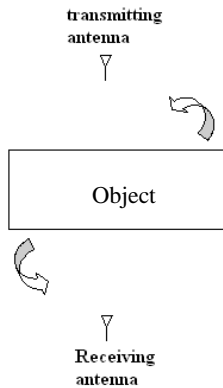
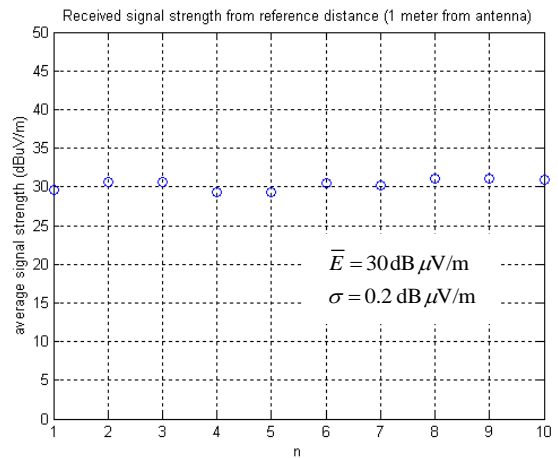


Fig. 12. Condition of measurement related to the orientation of an object

When the object was rotated in the anti-clockwise direction from 0° (horizontally) to 180° as shown in Figure 12, a minimum peak occurred at 105°, as shown in Figure 11. The strength of the signal was reduced linearly from 0° to approximately 90°. Then, the strength increase from 105° to 180°. When the object was rotated by 90°, the object was very close to the transmitting antenna and the receiving antenna. Both ends of the object acted as significant scatterers of the signal and acted as absorbing planes in diffraction [5]. The diffracted field would contribute to the strength of the received signal, since the diffraction occurred close to the transmitting antenna and the receiving antenna. However, when the object was rotated 180°, both ends of the object were far away from the transmitting antenna and receiving antenna, and the object had no influence on the strength of the signal. This is similar to the initial condition, i.e. before the object was rotated.

4. STRENGTH OF THE RECEIVED SIGNAL STRENGTH

4.1 Reference Distance (1 meter)



Note: Sample measurement on the n<sup>th</sup> day (The notation ‘n’ will be used in following figure.)

Fig. 13. Variation of the strength of the received signal for each measurement

Figure 13 shows the variation of the strength of the received signal which was measured 20 times/days at one meter from the antenna (reference signal strength). Figure 13 was used to study the repeatability of the data [6]. The reference distance (one meter) was used to normalize the path loss that occurred at one meter from the antenna so that only the propagation effects and the radiating (or far-field) effects are considered in the path loss [7]. The Rayleigh distance must be calculated to determine the boundary of the near field and the far field of the transmitting antenna:

$$R = \frac{2D^2}{\lambda} \tag{1}$$

By knowing the specifications of the antenna, Equation (1) can be rewritten as:

$$R = \frac{2l^2}{\lambda} \tag{2}$$

where  $l$  is the maximum length of the antenna. Therefore, the distance that was determined by Equation (2) is 1.0378 meter  $\approx$  one meter.

The mean value of the strength of the received signal that was obtained from 10 measurements at different times and reference positions from the antenna was around 30 dB  $\mu$ V/m. This value represents the strength of reference signal. Losses in the strength of the signal that occurred beyond this point were purely distance-dependent, due to the obstacles that blocked the signal, or interference from multi-path fading.

A log-periodic antenna received the signal at a height 0.8 m (desk level) above the floor. An average of 10 instantaneous samples was used to ensure that the propagation channel was stationary over time, standard procedure that is used in the literature [8]. Figure 13 shows that the signals fluctuated slightly, with a standard error of about 0.2 dB  $\mu$ V/m (Figure 13). Therefore, the strength of the signal is considered to be constant with time [8], and the correlogram in Figure 14 confirms this observation. Thus, it can be concluded that each position received almost the same amount of rays from the few fixed paths at each time.

The transmitting frequency bandwidth of a commercial WLAN is 2.4 to 2.4835 GHz. However, a narrower bandwidth, i.e. between 2.403 and 2.422 GHz was found from our measurements. In this work, the reference operating frequency was 2.413 GHz, the mid-band frequency.

Figure 15 represents the variation of the mean strength of the signal for all of the positions (positions 1 through 5) for 10 different sets of measurements.

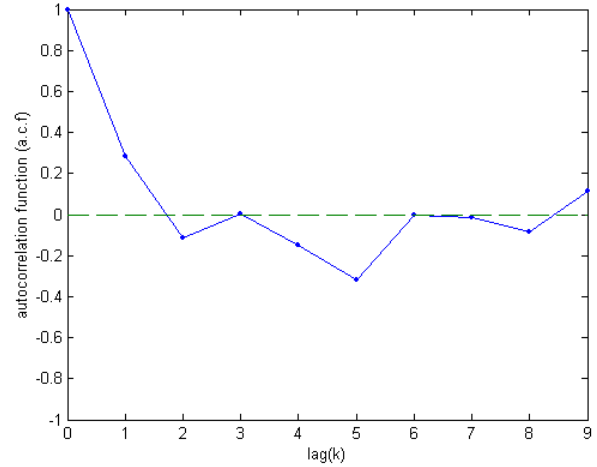


Fig. 14. Correlogram of the measured data at a reference distance of one meter

#### 4.2 Site A (Figure 4)

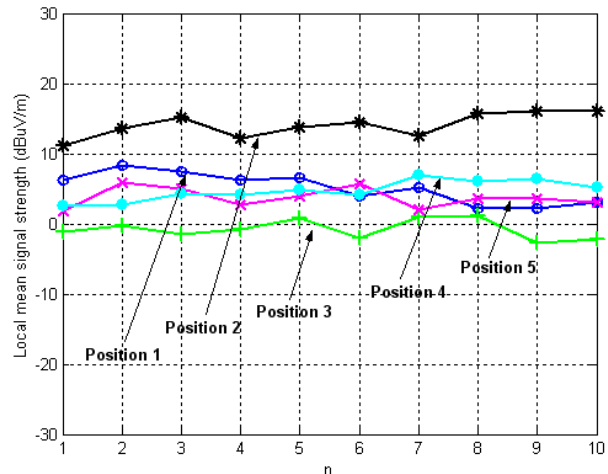


Fig. 15. Variation of the strength of the received signal at the time of each measurement at Site A

Table IV  
Statistical information and details of Site A

Position P, (m)	Mean signal strength, (dB $\mu$ V/m)	Standard error, (dB $\mu$ V/m)	Variability, (%)
P1, 15.667 m	14.08	0.5382	3.8
P2, 18.481 m	5.132	0.7004	13.6
P3, 19.001 m	0.776	0.4456	57.4
P4, 20.605 m	4.968	0.4560	9.2
P5, 23.499 m	3.771	0.4500	11.9

Five positions were selected in the NLOS region. Position 1 had the highest field strength because it was closest to the transmitting antenna; only a glass wall blocked it. Therefore,

the loss of signal strength at position 1 was due to both the glass wall [9] and the distance from the transmitting antenna. When the transmitted signal impinges on the surface of the

glass wall, the strength of the signal was distributed, causing a loss in the strength of the transmitted signal. Position 2 underwent conditions that were similar to those of position 1. However, position 2 was farther from the transmitting antenna than position 1 by about 2.8 m.

There was a significant obstacle for position 3, i.e., the concrete pillar that was in the path of the optical ray from the transmitting antenna. Before the ray penetrates into the room from the foyer, the glass wall also must be taken into account. As shown in Table 4, there was high variability at position 3 (57.4 %), which is logical considering the reception of multiple diffracted rays due to position 3's being located so close to the edge of the concrete pillar.

Position 4 and 5 were located adjacent to the concrete wall. For these positions, the reflected field from the adjacent wall was not considered because the distance of the receiving antenna from the concrete wall was very small compared to physical length of the receiving antenna of the receiving antenna. It is because the receiving antenna received the transmitted ray that penetrated through the glass wall before the ray impinged on the concrete wall. This explained the fact that the mean value of the strength of the received signal at position 3 was lower than the strength at all other positions. Position 3 was measured behind the concrete pillar, and it was very close to the concrete pillar. The insignificant and very

weak strength of the diffracted field [10] contributed to the strength of the field that was received at position 3. Diffracted rays and, reflected and scattered fields may exist at position 4, since the diffracted ray was considered to be the main contributor to the signal received at position 4. Therefore, the receiving antenna is in the NLOS condition.

4.3 Site B (Figure 5)

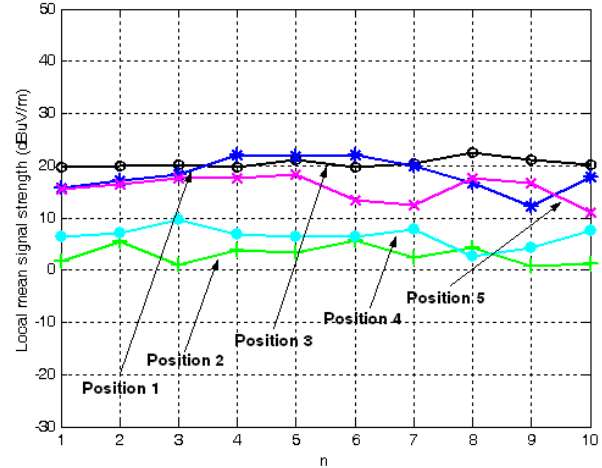


Fig. 16. Variation of the strength of the received signal at the time of each measurement at Site B

Table V  
Statistical information and details of Site B

Position P, (m)	Mean signal strength, (dB μV/m)	Standard error, (dB μV/m)	Variability, (%)
P1 (10.761)	18.35	1.0097	5.5
P2 (14.474)	2.98	0.5752	19.3
P3 (14.789)	20.48	0.2878	1.4
P4 (16.084)	6.48	0.6198	9.6
P5 (18.897)	15.66	0.7985	5.1

Actually, the characteristics of Site A and B were similar, as is apparent in Table 5. The arrangement of the furniture in both laboratories and their structures are similar. The entire channel that was occupied by the positions in Site B encountered similar propagation mechanism as Site A. However, there was a significant deviation between the signals received at Site A and B (Figure 16). Since all of the corresponding positions in Site B were closer to the transmitting antenna than the corresponding positions in Site A, the most probable explanation is the factor of distance.

The condition at position 1 of Site B is different from the condition at position 1 of Site A. To reach position 1 at Site B, the transmitted ray must penetrate a glass wall and a wooden

cabinet next to the glass wall. Therefore, the signal received at position 1 can be considered as NLOS signal.

Position 1 and position 2 are closer to transmitting antenna than position 3, but position 3 received the greatest mean signal strength. The main reason for this was the excessive losses caused by the wooden cabinet at position 1 and the concrete pillar at position 2. Position 2 received the weakest mean signal strength but had the highest variability among the positions at which signal strength was measured. The concrete pillar was thicker and denser than the wooden cabinet that blocked the signal position 1. The concrete pillar caused a high attenuation of the signal. Therefore, position 2 received a very weak signal from transmitting antenna by an indirect path. The condition at position 2 in Site B was similar



to the condition that occurred at position 3 in Site A. The multiple diffractions that occurred at the edge of the concrete pillar may have caused the multipath signal that was received at position 2, because position 2 was located very close to the edge of the pillar.

Positions 4 and 5 were located at the interior of Site B, which means that they received the mean signal strength after

the signal had travelled a longer distance. Position 4 was closer to the transmitting antenna than position 5, but a stronger signal was received at position 5 (Figure 16) because it was blocked on by the glass wall. Compare with position 4 that is blocked by the glass wall and the concrete pillar. Similar conditions existed at positions 1, 2, and 3, making the obstruction losses dominant.

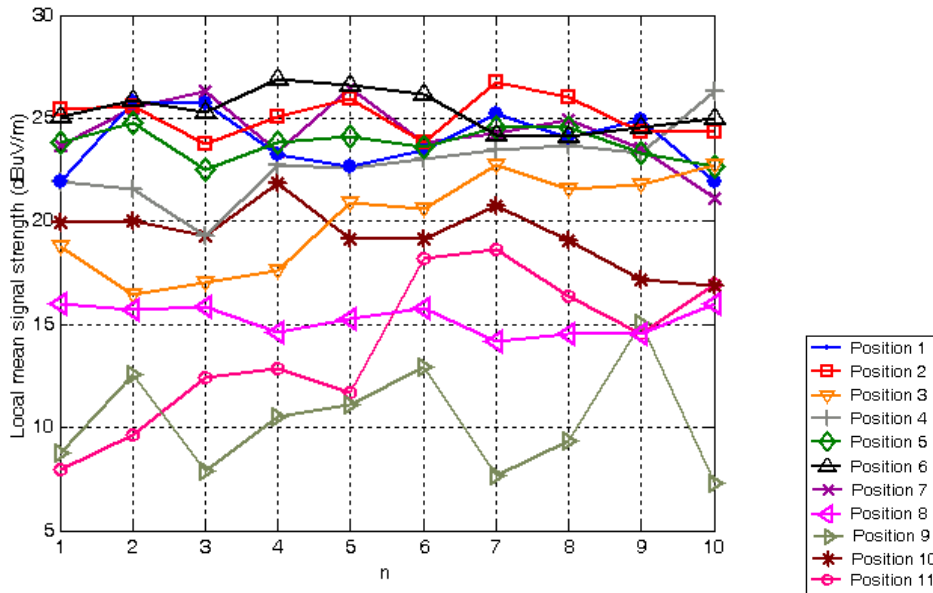


Fig. 17. Variation of the strength of the received signals each time a measurement was taken at Site C

Table VI  
Statistical information and details for Site C

Position P, (m)	Mean signal strength, (dB µV/m)	Standard error, (dB µV/m)	Variability, (%)
P1 (4.302)	23.9	0.4677	1.96
P2 (5.412)	25.11	0.3178	1.27
P3 (6.600)	20.01	0.7517	3.76
P4 (7.823)	22.78	0.5645	2.48
P5 (8.886)	23.76	0.2441	1.03
P6 (10.970)	25.37	0.3102	1.22
P7 (11.695)	24.30	0.5009	2.06
P8 (13.530)	15.25	0.2225	1.46
P9 (15.496)	10.30	0.8225	7.99
P10 (19.140 m)	19.33	0.4731	2.45
P11 (20.471 m)	13.93	1.1482	8.24

4.4 Site C (Figure 7)

The strengths of the received signals for all of the positions in Site C were in the LOS region. The performance of the channel in all the positions was expected to be

dependent on distance. However, Table 6 shows that the standard error percentages of the mean values (variability) of the strengths of the received signals at positions 3, 9 and position 11 are increasing more than those at the other positions in Site C. Positions 3, 9 and 11 had the largest percentages of variability, i.e., 3.8%, 8.0%, and 8.2%,

respectively. The ripple of the signal, which was caused by the interference between the direct signal and the scattered signal, as shown in Figure 17 (reflected or diffracted signal), contributed to these high values. Unfortunately, no values are given in the literature [11] to define the ripple signal. Comparatively speaking, the other positions did not have a severe fading problem, as indicated by their low percentages of variability, all of which were less than 3%. The fluctuation of the strength of the received signals may be due to the destructive superimposition of the scattered and direct signals. The effects of multiple reflections above third order [12] (when  $n > 3$  in Equation (3)) are too small in all of the positions in the LOS region and therefore can be ignored.

$$\theta = \frac{\pi}{2} + \alpha \tan^{-1}\left(\frac{2nh + ah_o}{d}\right) \tag{3}$$

where  $h_o = h_1 \pm h_2$  (Figure 18); the positive sign is used when the total number of reflections from the ceiling and the floor is odd, while the negative sign is used when the number is even; and  $\alpha = \pm 1$ , and, as a rule of thumb, the positive value is used when the first reflection occurs from the floor, while the negative value is used when the first reflection occurs from the ceiling. Equation (3) is illustrated by Figures 18 and 19.

Most of the positions gave almost zero readings after the third-order multiple reflections as shown from Figure 20(a) to

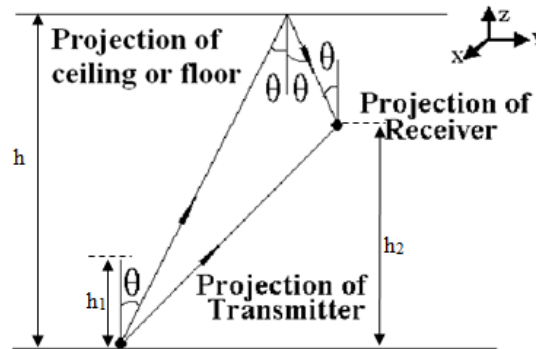


Fig. 18. Projection on the single floor

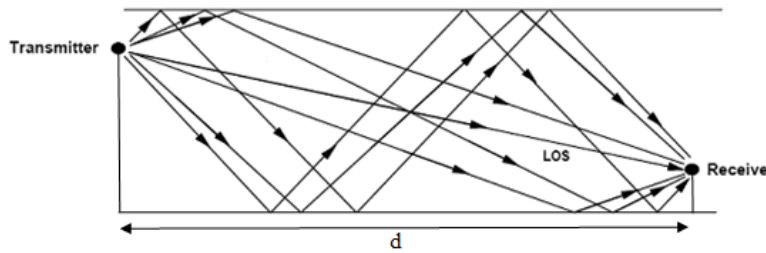


Fig. 19. View of multiple reflections from the floor and the ceiling.

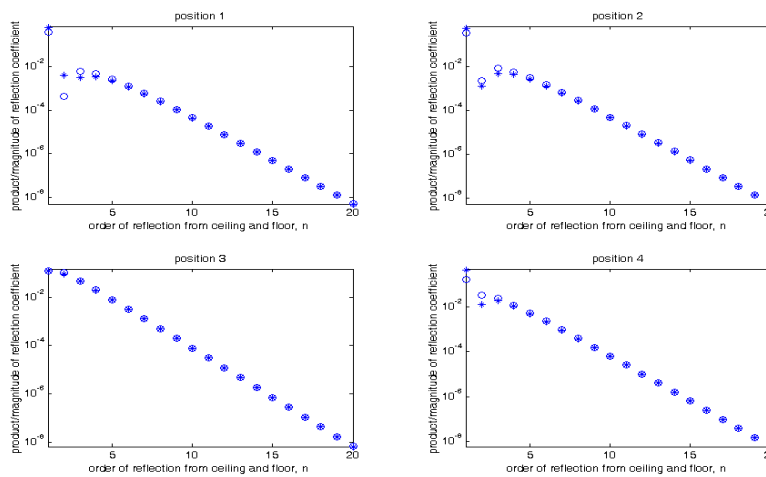


Fig. 20(a). Product/magnitude of reflection coefficients after some order of multiple reflections (Positions 1 to 4)

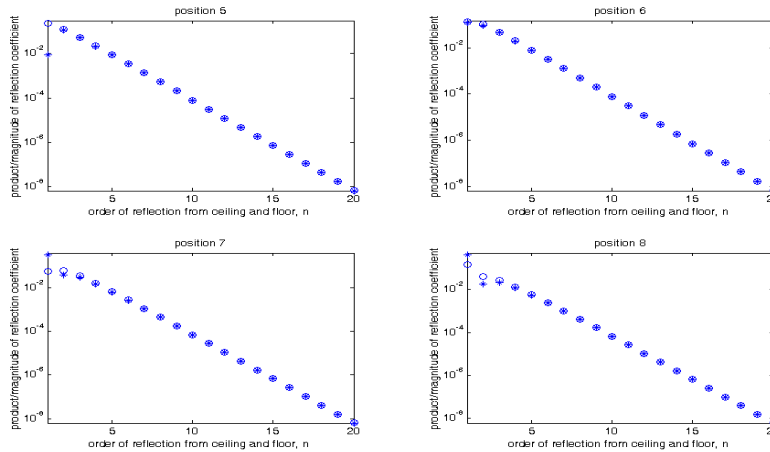


Fig. 20(b). Product/magnitude of reflection coefficients after some order of multiple reflections (Positions 5 to 8)

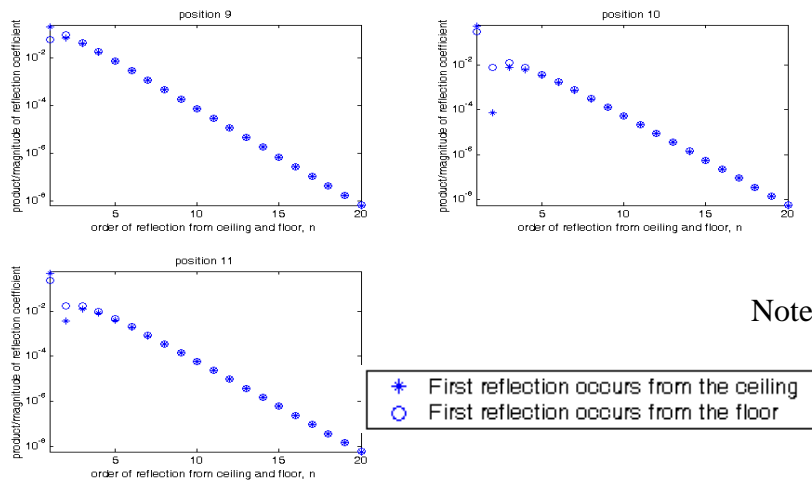


Fig. 20(c). Product/magnitude of reflection coefficients after some order of multiple reflections (Positions 9 to 11)

Figure 20(c). Most of the cases in Figure 20(a) to Figure 20(c) show that the strength of the multiple reflected signals above the third order can be omitted due to their small reflection coefficients.

#### 4.5 Site D (Figure 8)

The arrangement of furniture in Site D was not as crowded as in Site A and B. Therefore, the scattering effect was not significant in Site D. Even though there are soft partitions in Site D, they did not contribute to the problem of scattering in this site because the transmitting antenna was located higher than the soft partitions, and the receiving antenna was located some distance from the soft partitions. As a result, the ray path was not blocked by the soft partitions.

Compared to the signals received at Site A, B, C, and E, the signal received at Site D was very weak (i.e., 'buried' in the floor noise in spectrum analyzer and undetectable), as

shown in Figure 21 and Table 7. This occurred because the spectrum analyzer was unable to detect signals in some areas of Site D, e.g., where a corridor was formed like a tunnel. This is shown in the gray, shadow area in Figure 8. Multiple reflections occurred along the corridor, so the signal was weak, especially when the signal underwent multiple reflections that were higher than third order. The inner part of Site D in the shaded region (Figure 8) is the room after the corridor (Figure 10), and the spectrum analyzer results identified this as the 'blind spot' of the propagation of signal wave from the transmitting antenna (NLOS). Position 1 had the greatest mean signal strength among the positions. It is due to the factor of distance where position 1 is the closest position from the transmitting antenna. The vast difference of variability in position 2 compared with other positions was attributed to the blockage of an office (a glass and concrete wall). The NLOS signal was dominant at position 2, since the direct ray may not exist because it was blocked by a glass wall and a concrete wall in the office.

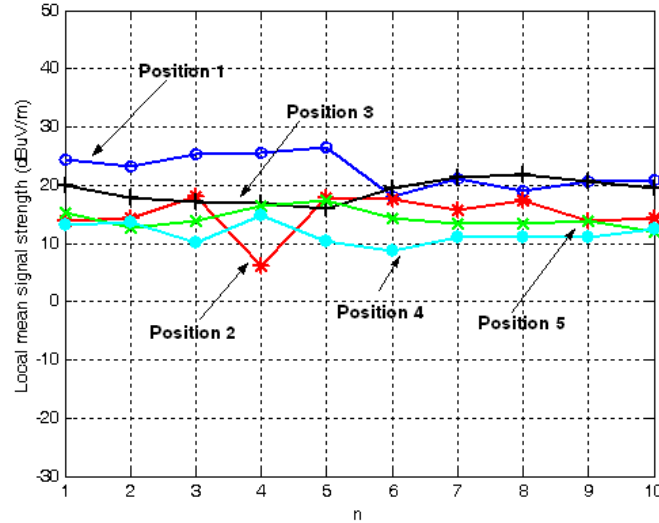


Fig. 21. Variation of the strength of the received signal each time a measurement was made at Site D

Table VII  
Statistical information and details of Site D

Position P, (m)	Mean signal strength, (dB $\mu$ V/m)	Standard error, (dB $\mu$ V/m)	Variability, (%)
P1 (2.334)	22.46	0.9386	4.2
P2 (6.518)	14.93	1.1084	7.4
P3 (7.029)	19.06	0.6280	3.3
P4 (9.860)	11.64	0.5819	5.0
P5 (10.277)	14.27	0.5357	3.8

#### 4.6 Site E (Figure 6)

Since Site C is not an NLOS region, the comparison among overall results in NLOS sites, i.e., Site A (Figure 15), B (Figure 16), D (Figure 21), and E (Figure 22) indicates that only Site D provided the best performance in reception. The distance factor was dominant in Site D since this site was located closer to the transmitting antenna than other NLOS sites, and the measured distance increased from position 1 to position 5.

The mean received signal for positions 1 through 5 in Site E are listed in Table 8. The mean signal strength in Site E seems lower than that in Site D, which indicates that Site E encountered greater loss even though its distance to the transmitting antenna was similar to that of Site D. Therefore, it can be deduced that the loss in Site E was not due to the distance factor. The geometrical location was the main reason for the loss. The orientation of the transmitting antenna and positions 2 through 6 resulted in the blockage of the direct

signal by a room. The fixed location of transmitting antenna caused the propagation of the direct ray signal to be blocked. Therefore, it can be concluded that no LOS ray was propagated into Site E, which can be considered as a shadowed region that do not receive any direct signal from the transmitting antenna.

The transmitted rays from the antenna undergo at least one interaction with an object or obstacle before being detected by the receiving antenna, because Site E is enclosed by a combination of a glass wall and a concrete wall. Therefore, the radiated rays from the source must penetrate these two obstacles before reaching Site E.

All the positions in Site E, except position 1, are blocked by a room. Position 1 received the transmitted (refraction) signal through a glass wall. Thus, most of the positions in Site E were in the condition of propagation between rooms [13]. Transmission through various materials or obstacles can be determined by using transmission coefficients in Equation (4):

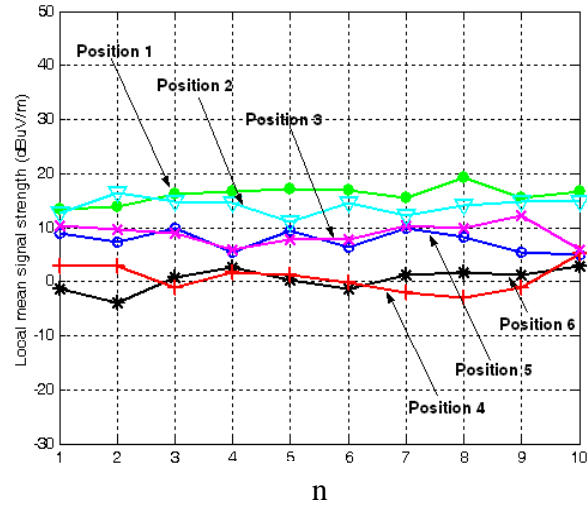


Fig. 22. Variation of the strength of the received signal each time a measurement was made in Site E

Table VIII  
Statistical information and details for Site E

Position P, (m)	Mean signal strength, (dB $\mu\text{V}/\text{m}$ )	Standard error, (dB $\mu\text{V}/\text{m}$ )	Variability, (%)
P1 (4.427)	16.09	0.5224	3.2
P2 (8.509)	14.00	0.4984	3.6
P3 (9.070)	8.92	0.6363	7.1
P4 (12.141)	0.64	0.8238	128.3
P5 (12.975)	7.58	0.6053	8.0
P6 (14.762)	0.45	0.6606	145.7

$$T_{||} = \frac{2 \cos \theta_i}{\sqrt{\epsilon_r \cos \theta_i + \sqrt{1 - \frac{1}{\epsilon_r} \sin^2 \theta_i}}} \quad (4)$$

where  $\theta_i$  is incidence angle of the incident wave, and  $\epsilon_r$  is relative permittivity of material for obstacle. However, transmission through a room may not be as simple as explained by Equation (4) because such transmission has higher uncertainty, such as the arrangement of obstacles with different types of materials [14] and the effect of mobile obstacles, such as a people moving inside the room [15]. Compared with other positions, the weaker received signals with extremely high variability at positions 4 and 6, as shown in Figure 22, were due to the blockage of the signals by the concrete pillar (Figure 6). Positions 4 and 6 were estimated to receive the signal after it had undergone two or three interactions with obstacles before reaching the receiving antenna. One concrete pillar and a room blocked position 6. In addition, position 6 received the signal where the distance of

the direct path from the measuring position to the transmitting antenna was the greatest among all of the positions in Site E. Position 4 was blocked by one concrete pillar and also by a room. However, it was relatively closer to transmitting antenna than position 6.

Even though Site E was relatively closer to the transmitting antenna than Site B, both of the sites also were located in an NLOS region; however a significant obstacle (a room) was blocking the direct ray signal in Site E. On the other hand, the concrete pillar that blocked positions 4 and 6 made its reception even worsen.

Repeat measurements of the same quantity are expected to yield results that are clustered around a particular value. If all major sources of errors [16] were taken into account, it is normal to assume that the remaining error must be the result of a large number of very small additive effects.

## 5. PATH LOSS DUE TO BUILDING MATERIAL

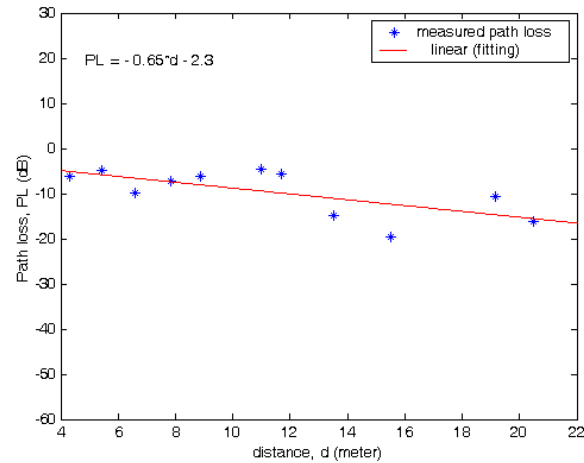


Fig. 23. Measured free space loss and its linear fitting model

Table IX  
Comparison between the measured obstruction loss and data from the literature [17]

Material	Penetration loss	
	Measured obstruction loss (dB)	Obstruction loss (dB) From the literature [14]
Glass	3.737	1.622
Door	4.023	2.261
Concrete wall	11.646	21.601
Thick wood	2.655	1.609

The measured obstruction loss was obtained by subtracting the losses due to obstacle and distance with free space or direct loss, as shown in Figure 23.

The measured obstruction loss had no good agreement with the obstruction loss stated in the literature [17] because the method used in the literature was in a free space measurement with a directional antenna (horn antenna). Higher directivity of the directional antenna could reduce problems due to multipath fading. It can ensure only that the direct signal through the material will be measured, while any multipath due to any other scatter present in the environments will be filtered out [17]. However, the transmitting antennas that were used in this study were in the form of omnidirectional antenna, which transmit the signal in all directions. Therefore, the multipath fading factor cannot be ignored in this study.

Another issue was that, the dimensions of materials used in the literature [17] were not well specified, so comparing the literature data with the measured obstruction loss may exhibit discrepancies. The types of materials used and their structures have an important role in determining the signal loss, because the dielectric properties and the number of layers of material determine the strength of the transmitted signal. The transmission coefficient equation given in Equation (4) is the

function of the dielectric constant. The dielectric properties must be considered in the determination of the signal loss in material. In addition, the structure of the material such as the number of layers, also must be taken into account because the number of layers will affect the multiple reflections within the layers and, thus, affect its penetration loss. It can be proved from the results that were measured for the concrete wall, which are listed in Table 9. The concrete wall showed the highest discrepancy between the measured obstruction losses with obstruction losses from the literature. This may due to the dissimilarity of the orientation of the structures inside the concrete wall.

In addition, these two different setups also will lead to discrepancies when the results are compared. The discrepancies are attributed to the cable loss or the systematic error in Spectrum Analyzer and in the vector network analyzer.

Even so, similarity can be observed by comparing the ratio of our measured obstruction to that in the literature, which was approximately two unless we were considering a concrete wall, because of the inhomogeneity and differences in the thicknesses of the walls.

## 6. CONCLUSIONS

In this project, several positions were selected in five measurement sites in the Division of Information Technology at Universiti Putra Malaysia, i.e., Site A to E. The study involved the investigation of signal performance throughout the building. The effects of the size and number of objects on signal reception were studied and found to have insignificant effects on the received signal. However, reception was still dependent on the area where all of the objects were located as well as the distances between the objects and the transmitting antenna. If an object was large and close to the transmitting antenna, the orientation of the object affected propagation loss.

Site A, B and E were affected by their distances from the transmitting antenna and the blockages due presence of a concrete wall and concrete pillars. In Site C, only propagation LOS was considered. All measured positions in Site C were solely distance-dependent. However, the signal scattering that was produced may cause inconsistencies in the strength of the signal received. Site D has a tunnel-like corridor, so multiple reflections from the ceiling and floor normally occurred. In this study, any reflections that occurred after the order exceeded  $n = 3$  were omitted.

Comparing the obstruction losses we measured with those in the literature, dissimilar patterns would have been observed due to different constructions. Material of obstacle used in a furnished indoor environment is crucial in signal coverage.

## Acknowledgments

The author thanks the staff members in the Division of Information Technology, University Putra Malaysia, for their assistance in setting up and conducting the measurements described here.

## REFERENCES

- [1] E. M. Cheng, Zulkifly Abbas, M. Fareq, K. Y. Lee, K. Y. You, and S. F. Khor. 2012. "Comparative Study Between Measurement and Predictions Using Geometrical Optics and Uniform Theory of Diffraction for Case of Non-Line-of-Sight (NLOS) in Indoor Environment." *Wireless Pers Commun.* DOI 10.1007/s11277-012-0931-9 (In Press)
- [2] Nešković, A., Nešković, N., Paunović, D., 2000. "Modern Approaches in Modeling of Mobile Radio Systems Propagation Environment". *IEEE Communications Surveys*, Third Quarter, pp. 2-12.
- [3] Zhong Ji, Bin-Hong Li, Hao-Xing Wang, 1999. "A New Indoor Ray-Tracing Propagation Prediction Model" *International Conference on Computational Electromagnetics and Its Applications 1999, (ICCEA '99)*, pp. 540-542.
- [4] Ernst Bonek. "Digital Mobile Radio Towards Future Generation Systems: COST 231 Final Report: Tunnel, Corridors, and other Special Environments". Technical University of Vienna, Austria, 2010, pp. 190-207.
- [5] Saunders, S.R. 1999. "Antennas and propagation for wireless communication systems." New York: John Wiley & Sons Publisher.
- [6] Bentley, J.P., 1995. "Principles of Measurement Systems". Pearson Education Asia (Pte) Ltd., pp. 14, 26
- [7] Chung, K.W., Jonathan, H.-M. Sau, and Murch, R.D, 1998. A new empirical model for indoor propagation prediction." *IEEE Transactions on Vehicular Technology*, vol. 47, no. 3, pp. 996-1001.
- [8] Zhong, Ji, Li, B.H., Wang, H.X., Chen, H.Y., Sarkar, T.K., 2001. "Efficient Ray-Tracing Methods for Propagation Prediction for Indoor Wireless Communications." *IEEE Antennas and Propagation Magazine*, vol. 43, no. 2, pp. 41-49.
- [9] Fiacco, M., Parks, M., Radi, H., and Saunders, S. R, 1998. "Final Report: Indoor Propagation Factors at 17 GHz and 60GHz." Center for Communication Systems Research, University of Surrey on behalf of the Radiocommunications Agency.
- [10] Paolo Bernardi, Renato Cicchetti, and Orlandino Testa, 2004. "An Accurate UTD Model for the Analysis of Complex Indoor Radio Environments in Microwave WLAN Systems." *IEEE Transactions on Antenna and Propagation*, vol. 52, no. 6, pp. 1509-1520.
- [11] Chang, C.W., Stanley Mak, M. Neve, and G. Rowe., 2003. Part IV Project Report, Final Report: Radiowave Propagation Modeling using the Uniform Theory of Diffraction. School of Engineering, Department of Electrical and Electronic Engineering, The University of Auckland.
- [12] Li, B. H., Zhong, Ji, Wang, H.X., Chen, H.Y. and Zhau, Y.G. "A New Indoor Ray-Tracing Propagation Prediction Model." Dept. of Electronic Engineering Shanghai Jiao-Tong University, Shanghai, China.
- [13] Philip Nobles, 1998. "Final Report: A Study Into Indoor Propagation Factors at 17 GHz and 60 GHz." Communication Research Group, University of Wales Swansea.
- [14] Pecha Echač P. and Klepal, M. "Empirical Models for Indoor Propagation in CTU Prague Buildings." *Radioengineering*, (2000), vol. 9, no. 1, p. 31-36.
- [15] Huo Hongwei, Shen Wei, Xu Youzhi, and Zhang Hongke. 2009. "The effect of human activities on 2.4 GHz radio propagation at home environment." 2nd IEEE International Conference on Broadband Network & Multimedia Technology, 2009. IC-BNMT '09. pp. 95-99.
- [16] Caleb Phillips, Douglas Sicker, and Dirk Grunwald. 2012. "Bounding the Practical Error of Path Loss Models." *International Journal of Antennas and Propagation*. Volume 2012 (2012), Article ID 754158, 21 pages.
- [17] Mohammed, Y. E., Abdallah, A. S., and Liu, Y. A., 2003. "Characterization of Indoor Penetration Loss at ISM Band." *Asia-Pacific Conference on Environmental Electromagnetics CEEM' 2003*, Hangzhou, China.